energies

MDPI

Article

Impact Assessment of Electric Vehicle Charging in an AC and DC Microgrid: A Comparative Study †

Rémy Cleenwerck [1,2,*,‡], Hakim Azaioud [1,‡], Majid Vafaeipour [2], Thierry Coosemans [2] and Jan Desmet [1]

[1] EELab/Lemcko, Deptartment of Electromechanical, Systems and Metal Engineering, Ghent University, 8500 Kortrijk, Belgium; hakim.azaioud@ugent.be (H.A.); janj.desmet@ugent.be (J.D.)
[2] EVERGi, MOBI Research Centre & ETEC Deptartment, Vrije Universiteit Brussel, 1050 Brussel, Belgium; majid.vafaeipour@vub.be (M.V.); thierry.coosemans@vub.be (T.C.)
* Correspondence: remy.cleenwerck@ugent.be
† This paper is an extended version of our paper published in 35th International Electric Vehicle Symposium and Exhibition (EVS35), Oslo, Norway, 11–15 June 2022.
‡ These authors contributed equally to this work.

Abstract: This paper presents an in-depth comparison of the benefits and limitations of using a low-voltage DC (LVDC) microgrid versus an AC microgrid with regard to the integration of low-carbon technologies. To this end, a novel approach for charging electric vehicles (EVs) on low-voltage distribution networks by utilizing an LVDC backbone is discussed. The global aim of the conducted study is to investigate the overall energy losses as well as voltage stability problems on DC and AC microgrids. Both architectures are assessed and compared to each other by performing a power flow analysis. Along this line, an actual low-voltage distribution network with various penetration levels of EVs, combined with photovoltaic (PV) systems and battery energy storage systems is considered. Obtained results indicate significant power quality improvements in voltage imbalances and conversion losses thanks to the proposed backbone. Moreover, the study concludes with a discussion of the impact level of EVs and PVs penetration degrees on energy efficiency, besides charging power levels' impact on local self-consumption reduction of the studied system. The outcomes of the study can provide extensive insights for hybrid microgrid and EV charging infrastructure designers in a holistic manner in all aspects.

Keywords: electric vehicles; LVDC backbone; DC microgrid; power quality; converter efficiency

Citation: Cleenwerck, R.; Azaioud, H.; Vafaeipour, M.; Coosemans, T.; Desmet, J. Impact Assessment of Electric Vehicle Charging in an AC and DC Microgrid: A Comparative Study. *Energies* **2023**, *16*, 3205. https://doi.org/10.3390/en16073205

Academic Editor: Juri Belikov

Received: 6 March 2023
Revised: 31 March 2023
Accepted: 31 March 2023
Published: 2 April 2023

1. Introduction

The increasing popularity of low-carbon technologies, such as electric vehicles (EVs), has brought attention to the potential impact they may have on the distribution networks (DN) [1,2]. Due to their stochastic nature, there is a growing concern among DN operators about how the DN could cope with these uncertainties within the grid. Conventional methods to charge EVs on a low-voltage DN involve the use of AC/DC converters. These conversion stages lead to energy losses [3] and can also cause power quality issues [4]. Moreover, it is expected that as more EVs are connected to the grid, DN will be confronted more frequently with violations of grid standards [5]. Therefore, this study presents a novel approach while considering a real-world distribution network to enable large-scale EV charging in a residential context. Instead of connecting each individual EV-charging station to the DN, the proposed method introduces a low-voltage DC (LVDC) backbone. The backbone is described within the present work as an extension of the already existing AC microgrid to which all low-carbon technologies are connected. Thus, the need for individual AC/DC converters is reduced, leading to a decrease in energy losses and material cost.

Due to their stochastic nature, we define these low-carbon technologies (e.g., EVs, photovoltaic (PV) systems and battery storage systems (BESS)) as stochastic distribution grid exchangers (SDGE). Since the studied network includes house-units featuring PV

systems, the analysis is carried out for different PV penetration levels towards identifying the synergy between both EVs and PV systems. In this respect, an assessment of EV charging for a residential DN is compared to a hybrid AC/DC microgrid. Based on a probabilistic approach, different power quality parameters (i.e., voltage limit violations and voltage unbalance factor) are examined. Furthermore, the comparative study discusses the losses occurring in both topologies and analyses the potential benefits.

Despite the growing interest in EVs and RES, no studies were found that specifically compared their integration via both microgrid architectures. Therefore, this paper makes a unique contribution to the field by comparing the integration of SDGEs on a low-voltage DC microgrid versus an AC microgrid. To perform a comprehensive sensitivity analysis, various penetration levels of EVs and PV systems were examined. Consequently, the main contributions of the present study can be summarized as:

1. An analysis of the impact of various EV and PV penetrations on the voltage profiles is performed based on the probability distributions of the arrival times and state-of-charge (SoC) conditions upon arrival. Results are assessed for compliance with the EN 50160 standard.
2. The impact of the voltage profiles on the PV curtailment losses on the LVDC backbone is assessed. This is due to the fact that all PV systems are directly connected to the branch without an intermediate DC/DC converter. Branch voltages are set in the central DC/DC converters to follow the maximum power point voltage of the PV systems. The stochastic EV demand and solar irradiance may cause the voltage profile along the network to fluctuate, resulting in PV curtailment losses.
3. The different losses to distinguish the cable losses and converter losses in both architectures are extensively investigated.
4. The voltage unbalance factor (VUF) for the worst-case scenario with different EV penetration levels, the correlation with the node losses and the VUF violation thresholds will all be assessed and identified.

The remainder of the paper is as follows: first, Section 2 provides a global overview of the state of the art for (i) the LVDC backbones and (ii) research related to the influence of EVs on DN. Hereafter, Section 3 discusses the grid specifications, the used datasets and the modelling of the PV systems and BESS. Next to this, the performed power flow analysis is discussed including the simulation variables. Section 4 addresses the obtained results of the power flow analysis, i.e., the impact of the simulation variables on (i) the voltage profiles, (ii) the energy losses and (iii) the voltage unbalance. Herein, a distinction is made between results associated with the AC part on the one hand and results related to the LVDC backbone on the other hand. Finally, key observations are summarized. Overall conclusions are drawn in Section 5 and future research directions are provided in Section 6.

2. Literature Review

2.1. Research in the Field of LVDC Backbones

Nowadays, applications of LVDC at the distribution level are actively researched. Depending on the voltage level, LVDC microgrids have several advantages, such as (i) higher power transfer capability, (ii) better controllability, and (iii) improved converter efficiency. Many household appliances and SDGEs operate on DC, which implies that a DC microgrid could drastically reduce the required amount of converters [6]. As converters contain semiconductors and capacitors which are prone to failure, the reliability and lifetime could be increased. Moreover, the elimination of a converter stage would lead to an increase in system efficiency [7]. Notwithstanding all these advantages, certain challenges, such as expensive protection devices or the lack of standardisation, prevent the application of DC microgrids on a large scale. A radical shift to LVDC would necessitate great investments in both capital and time. However, a hybrid AC/DC structure would be more feasible and could pave the way for a gradual transition [8].

In that context, previous research has demonstrated that an LVDC backbone architecture benefits from multiple advantages for energy communities centred on a single

feeder [9]. LVDC backbones consist of aggregated PV systems and a central BESS. The latter connects the LVDC backbone through a central DC/AC inverter to the point of common coupling (PCC) of the AC microgrid, further referred to as the single point of connection (SPoC). Another finding of the referred study [9] is that conversion losses in the proposed architecture can decrease significantly—up to 12 percentage points—compared to a traditional AC microgrid. This is mainly driven by the favourable system voltages which led to a lower voltage ratio and hence lower conduction and switching losses of the converter. Non-proportionality between the system scale and the switching and core losses strengthens the advantage of an LVDC backbone compared to a traditional AC DN.

Extending the LVDC backbone with distributed EV chargers is a solution to increase the PV self-consumption (SC) and hence improve the converter efficiency. Furthermore, this is a solution to circumvent the aforementioned power quality issues and reduce the use of raw materials. The environmental impact analysis conducted in [10] made a comparative evaluation between onboard and off-board chargers using a life cycle analysis framework and methodology. They concluded that a DC charger is superior in terms of environmental and economic impact, which is mainly due to the scaling effect and higher efficiency of DC charging. It should be noted that the additional energy consumption caused by the weight of the onboard charger was not considered in the analysis, which may further increase the benefits of DC charging. While that study specifically focused on the advantages of fast DC charging, it is expected that conventional charging on an LVDC backbone may also be beneficial due to the reduced number of converter stages and the use of a centralized AC/DC converter instead of multiple distributed converters.

A comparative study [11] of an AC and DC microgrid including EV chargers has been performed in terms of efficiency and voltage profiles. Key findings of that research demonstrate that an LVDC system is more favourable in case of radial DN, while it is only slightly more efficient in the case of meshed grids. Concerning the voltage profile, LVDC systems exhibit smaller voltage deviations regardless of the topology. Although, one should note that it is not clear from that study how the converter losses were assessed. Another aspect is the simulation's time horizon, which is restricted to 24 h. It should also be noted that neither renewable energy sources (RES) nor energy storage systems have been taken into account, which are crucial to consider in contemporary DN. Reference [12] is, in contrast, very promising. Here, researchers tackle the subject from another point of view where the AC and DC nanogrids are seen from a building level. Therefore, their comparison distinguishes the usage of a 48 V_{DC} versus a 380 V_{DC} and demonstrates that a 380 V_{DC} nanogrid can outperform both the AC nanogrid and the DC nanogrid operating at 48 V_{DC}. However, their approach focuses on the application of an LVDC on building level. Gerber et al. [13] executed a similar comparison of efficiency losses but on a different scope, i.e., in commercial buildings and not on a distribution grid level. To the best of the authors' knowledge, no research has been published where an exhaustive comparative analysis is made on DN-level between an LVDC backbone and a traditional LVAC architecture with distributed EV chargers.

2.2. Research Related to the Impact of EVs

Accordingly, the focus of this article is to assess the energy efficiency and power quality aspects between the two architectures for varying EV charging powers and PV system sizes. The rapid growth of EV adoption forms a potential opportunity for mitigating the power quality problems caused by the increased reverse power flows of RES in DN [14,15]. Nonetheless, the inherent spatiotemporal stochasticity of these assets may cause violations of certain power quality indices [16]. According to the European EN 50160 standard [17], the 10 min mean rms voltage deviation should not exceed $\pm$10%, and the voltage unbalance factor (VUF) should remain below 2% for 95% of the time. These grid limitations are the subject of several studies involving EVs [18–20].

Reference [5] analyses the grid voltages on a Flemish DN with an EV penetration degree of 100% with only single-phase connected households. These are alternately con-

nected between the three phases and the neutral conductor. It is assumed that the EV charging power is 3.3 kW, while the PV penetration degree amounts to 35% among the connected dwellings. This heavily unbalanced grid state causes the voltage magnitude to drop drastically and attain minima of 0.75 pu. Consequently, the maximum VUF reaches up to 5%, and it can be stated that the grid is not compliant.

Held et al. [21] studied the impact of EV charging on typical German grids while focusing on the voltage stability and the thermal limitations of a distribution cable. A distinction is made between rural and suburban grids with different transformer sizes and feeder lengths, including the cable cross section. No VUF limit was violated for all the studied cases, and the highest noticeable unbalance was measured in a suburban grid with the longest feeder lengths, which was intuitively expected. However, due to a lack of data from the transformer, voltage unbalances on the low-voltage side could not be taken into account. Nonetheless, the study highlights the voltage stability as the main critical factor for EV integration in low-voltage DN. For high EV penetrations, the minimum voltage was close to the limit or even exceeded it in urban and suburban grids with, respectively, the longest feeder and the highest number of household connections. However, no RES were considered within their study, which differentiates it from our contribution.

A study from the Netherlands [22] pointed out that older networks will especially suffer from congestion issues, such as undervoltage. The study took into account different integration scenarios for EVs, PV systems and heat pumps. Authors from [22] suggested some actions, such as augmenting the cable capacity, to solve the congestion issues. In contrast, our contribution presents a more durable solution by adding a cable that operates as a unipolar LVDC backbone where PV systems, BESS and EVs could be connected. While the scope of the presented work does not consider harmonic distortion, Marah et al. [23] highlight the importance of mitigating the adverse impact on the overall network's power quality due to electric vehicle charging stations. Similarly, the impact of harmonic currents caused by electric vehicles is assessed in [24], demonstrating that the power quality could be jeopardized and thus influence the degradation of the low-voltage distribution transformers. Therefore, they proposed an optimal harmonic power flow in order to restrain the harmonic distortion within the standard limit.

3. Methodology

For this study, a representative three-phase four-wire LV radial DN of a semi-urban area with a balanced mix between detached and semi-detached house-units is utilised. The start of the studied DN is considered at the PCC, i.e., LV-side, of the distribution transformer, as depicted in Figure 1. Here, Figure 1a represents the topology for the power flow simulations in AC, while Figure 1b illustrates the LVDC backbone. Note that the LVDC backbone is connected through an SPoC to the transformer's LV-side, as shown in the top part of Figure 1b. In contrast to the conventional AC method where multiple feeders depart from the LV busbar of the transformer (i.e., PCC), the proposed LVDC backbone consists of three common DC-buses. At each of these buses, multiple DC/DC converters are connected, consisting of a cluster of PV systems and EV chargers distributed on a DC-branch. Both, the DC-buses and DC-branches are unipolar but are operating on a different voltage level. The DC-branch is operating on the maximum power point (MPP) voltage which varies between 180 V and 325 V, while the DC-bus operates at 700 V in order to avoid extensive cable losses.

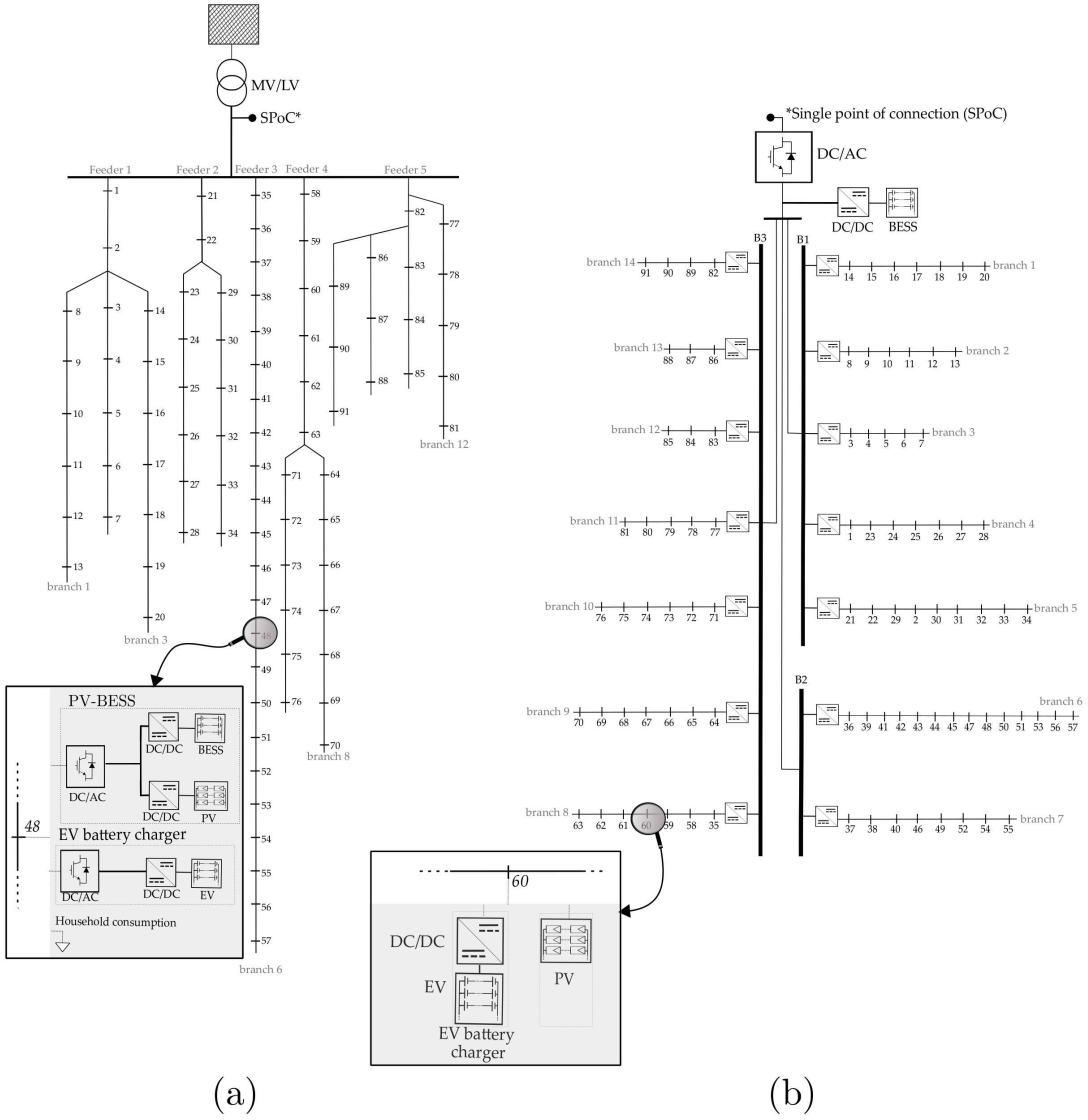

Figure 1. Line diagram of the studied LV DN with a detailed view of the connection of the load and SDGEs, with (**a**) the conventional approach and (**b**) the proposed LVDC backbone.

To this end, house-units were modelled in the conventional—AC microgrid—case, each with an individual EV charging station, a PV system and a BESS. In each, the EV charging station and the PV-BESS are provided by a separate DC/AC converter. Accordingly, PV systems and the corresponding BESS are connected to the same AC/DC inverter via an individual DC/DC converter, as highlighted in Figure 1a, and every DC/DC converter from the PV systems includes a maximum power point tracking (MPPT), whereas the suggested approach—LVDC backbon—considers distributed PV systems to be directly connected on the DC-branch via a centralized MPPT to the DC-bus. Here, a community BESS is introduced in order to achieve a fair comparison between the two cases while reducing the number of converters.

We delineate the analysis to a residential area with single-phase connected house-units. Consequently, the maximum charging rates are set to 7.4 kW [25], and the installed capacity of PV systems is limited to 5 kVA [26]. In order to observe the consequences of both (i) EVs and (ii) PV systems, simulations are subject to penetration levels in increments of 25% up to a penetration level of 100%, where the 0% case (i.e., only consumption profiles) is considered as the reference.

3.1. Datasets

Several datasets were used for the study. For instance, historical consumption profiles (with a 15 min resolution) were taken from a dataset of 1422 residential consumers provided by Fluvius cvba. The pre-processing of the dataset is part of previous research carried out by Claeys et al. [27]. However, the 91 selected consumption profiles are subject to random selection in which the annual consumption ranges between 1000 kWh and 5000 kWh, thus ensuring the inclusion of small- and medium-sized consumers as specified in [28]. EV profiles are generated from real-world arrival and departure times obtained from ElaadNL [29]. The probability densities used to determine the arrival times and the initial SoC of the EVs are depicted in Figure 2a,b.

A dynamic charging process is applied to avoid overcharging degradation. The charging process consists of a constant current (CC) stage followed by a constant voltage (CV) stage based on the approach presented in [30]. Here, the CV stage reduces the risk of the battery voltage violating its threshold, while the battery's terminal voltage v_{charge} and current i_{charge} during the CC stage is calculated as follows:

$$v_{charge}(t) = V_{OC}(SoC(t)) - R \cdot i_{CC} \quad (1)$$

$$i_{charge}(t) = i_{CC} \quad (2)$$

$$\textbf{subject to } t < t_s$$

where R is the battery resistance (assumed to be constant [31]), and t_s denotes the moment for which the terminal voltage equals the predefined maximum voltage V_{CV}. Open circuit voltage and the current during the CC stage, respectively, V_{OC} and i_{CC}, are expressed in Equations (3) and (4):

$$V_{OC}(SoC(t)) = E_0 - \frac{K}{SoC(t)} + A \cdot exp(-BQ(1 - SoC(t))) \quad (3)$$

$$i_{CC} = \frac{V_0 - \sqrt{V_0^2 - 4P_B(0)R}}{2R} \quad (4)$$

with E_0 representing the battery constant voltage, K the polarization constant and Q the nominal battery capacity. Parameters A and B represent the amplitude and the time constant inverse in the exponential zone of the $V_{charge} = f(SoC)$ curve. Finally, $V_0 = V_{OC}(SoC(0))$ and $P_B(t)$ are the battery power profile. Once the voltage reaches the predefined maximum voltage level V_{CV}, Equation (5), the charging stage switches from CC to CV.

$$V_{CV} = V_{OC}(SoC(t)) - R \cdot 3600 \cdot Q \cdot \dot{SoC}(t) \quad (5)$$

In contrast with Equations (1) and (2), the following expressions can be used for determining the voltage and current values during the CV stage:

$$v_{charge}(t) = V_{CV} \quad (6)$$

$$i_{charge}(t) = 3600 \cdot Q \cdot \dot{SoC}(t) \quad (7)$$

$$\textbf{subject to } t \geq t_s$$

The obtained dynamic voltage and current charging curves as well as the SoC curve are presented in Figure 2c,d. Note that electrical circuit models are usually determined for individual cells, while in this study battery packs consist of multiple cell strings connected in series. Therefore, a conversion is applied. The conversion methodology and parameters used for modelling the dynamic charging process can be found in [30] and are based on the Nissan Leaf's battery pack.

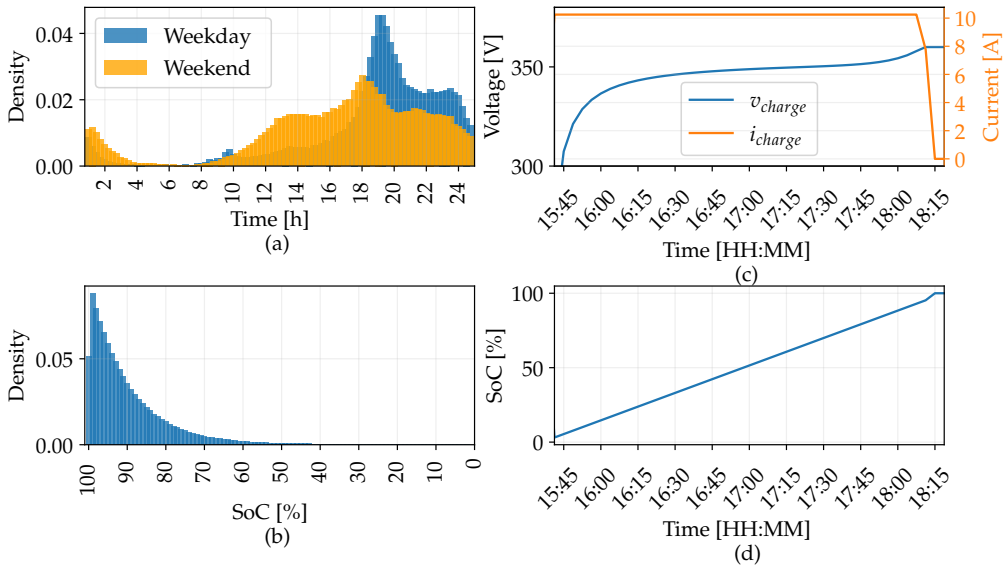

Figure 2. Probability densities and dynamic charging curves, with: (**a**) the distribution of arrival times for weekdays and weekends; (**b**) the SoC upon arrival at destination. Both right panels are representative of a randomly selected day with: (**c**) the charging voltage and current; (**d**) the respective SoC curve.

A summary of the networks' specifications is given in Table 1. Lastly, climate data provided by the Belgian Royal Meteorological Institute are used as input for modelling the generated power by the PV system. These data consist of wind speed, global irradiance and temperature, all having a resolution of 15 min (matching the consumption data).

Table 1. Summary of the grid specifications.

Description	Values
Transformer rating	250 kVA
Grid voltage	3 × 400 V + N
DC Backbone voltage	700 V
Distribution cable	EAXeVB 4 × 150 mm^2
Connection cable	EXVB 4 × 16 mm^2
No. of house-units	91
Max. feeder length	400 m
Distance to junction	[8,. . ., 15] m
Yearly consumption	[1000,. . ., 5000] kWh

3.2. PV-BESS Modelling

It is important that the PV model is accurate in estimating the operating point, especially when the voltage level V_{PV} deviates from the MPP voltage V_{MPP}. Therefore, the generated power of the PV system is estimated by a single-diode cell model [32] and the parametrization is based on the SAM module database [33]. Further, the implemented PV system uses a Yingli YL-230P-29b module. No local optimization is introduced, implying that all tilt angles and azimuths are considered to be fixed with, respectively, 35° as tilt and 180° for the azimuth. The in-plane irradiance is calculated following the methodology described in [34]. Finally, the amount of solar panels in series and parallel is configured as a function of the total annual consumption (E_{load}) as presented in Table 2.

Table 2. PV sizing as a function of the total load demand.

Total Annual Load Demand E_{load} [kWh]	Modules in Parallel	Modules in Series	Total Power of Installed PV $P_{pv,tot}$ [kWp]
$0 < E_{load} \leq 2435$	1	9	2.07
$E_{load} > 2435$	2	9	4.14

To extract the maximum power from the PV system, voltage levels are controlled by a DC/DC converter, thus corresponding to the actual V_{MPP}. However, in the case of an LVDC backbone, PV systems are directly connected to the DC-branch which operates at the MPP voltage. As a consequence, the number of conversion stages between the local EV-charging stations connected on the same branch and the PV systems is reduced. This leads to a reduction in the number of converters and higher energy efficiency. However, due to local voltage deviations on the DC-branch, this inevitably results in a reduction of the extracted power which will be quantified in the analysis.

Finally, battery losses and voltage variations as a function of the SoC have been taken into account using the method described in [35]. The battery management strategy aims to maximize the SC, whereas BESS specifications and a sizing approach can be found in [9].

3.3. Power Flow Analysis

This research aims to obtain results for a set of diverse scenarios, therefore different modes of EV charging are considered, ranging from domestic charging (2.3 kW) to the max allowed single-phase charging (7.4 kW). It is assumed that the load distribution of the house-units is symmetrically connected to the distribution cable (i.e., house-unit 1 is connected to L1-N, house-unit 2 to L2-N, house-unit 3 to L3-N and house-unit 4, again to L1-N, etc.), hence resulting in voltage unbalance [36]. Allocation of the charging stations takes place randomly but in accordance with the allocation of PV systems. Further, as previously mentioned, the behaviour pattern of charging hours is also assumed. Note that the EV charging process is uncoordinated. In order to include the seasonal effects of the PV yield and the load demand, the simulation is performed over one year. Simulations are performed within an OpenDSS-Python environment. Therefore, the DN is modelled in OpenDSS [37], while the actual time-series power flow analyses are performed in Python through the OpenDSS COM interface, as presented in [38]. The method adopted for the modelling of the cables is described in [39]. Results for the conventional method are obtained through a steady-state power flow analysis performed on a yearly profile with a 15 min resolution, where the complex power injection at bus i is given by

$$S_i = P_i + jQ_i \tag{8}$$

Expressions for the active and reactive power injections at bus i, respectively P_i and Q_i are obtained by identifying the real and imaginary part of the power injection S_i from Equation (8), yielding

$$P_i = |V_i| \sum_{j=1}^{N} |V_j| (Y_{ij} \cos(\theta_i - \theta_j)) \tag{9}$$

and

$$Q_i = |V_i| \sum_{j=1}^{N} |V_j| (Y_{ij} \sin(\theta_i - \theta_j)) \tag{10}$$

where $|V_i|$ is the voltage magnitude, θ_i is the voltage angle, and Y_i is the admittance at a given bus i. Note that $\forall\, i \in N$, $i = 1, \cdots N$. Using Equations (9) and (10), various scenarios are compared by evaluating the impact of EVs and PV penetration degrees ranging from 0% to 100%. Table 3 presents a summary of the input variables for the algorithm. In order to quantify the discrepancy between the conventional method and the proposed approach,

simulations for the LVDC backbone are derived from the reference case of the conventional method (i.e., 0% penetration level for the EVs and PV systems).

Table 3. Overview of the simulation variables.

Description	Values	Unit
EV penetration	ℸ{0; 25; 50; 75; 100} *	[%]
PV penetration	ℸ{0; 25; 50; 75; 100} *	[%]
Charging power	ℸ{2.3; 3.7; 5.8; 7.4} †	[kW]

* ℸ {a, b} denotes a discrete uniform distribution between a and b. † Charging rates derived from [25], as well as applied by the Belgian DSO Fluvius cvba [40].

For this purpose, the reference scenario provides a quantification of the load losses incurred by each house-unit, while conversion and cable losses are obtained from a backward–forward sweep algorithm in Python. The implemented conversion loss models are based on previous work [9], where a distinction is made, respectively, for the conventional and proposed method. Finally, the DC/AC converter of the EV charging station is modelled as a single-phase full bridge active rectifier. To conclude this section, all calculations are performed on a computer with Intel(R) Core(TM) i7-8850H CPU with a speed of 2.6 GHz and an installed RAM of 16GB.

4. Results

This section describes the results obtained for the respective criteria. Nevertheless, comparisons between the two situations cannot be directly made as the application differs for both the conventional and proposed method. Results for voltage deviations are consequently divided into two parts, namely an AC part and a DC part.

4.1. Voltage Profiles — Partim AC

Figure 3 provides the probability density functions of all voltage profiles from each individual bus of the LV DN. Voltage magnitudes are expressed per unit (p.u.) on the x-axis, where the normalised 1 p.u. represents 230V, whereas the normalised density probabilities are reflected on the y-axis. These probabilities are represented by Gaussian distributions. Results are shown for the 85 combinations of penetration levels for EVs and PV systems. Herein, columns iterate through the EV levels, and rows iterate along the PV penetration degrees. Both iterations are performed in steps of 25%, starting at the reference case of 0%. This reference case is indicated in all subplots by a grey-shaded histogram, while the colours refer to the charging rates. The obtained outcome is representative for the conventional charging of electric vehicles on an LV DN. Hence, this is valid for both cases, where PV is present or omitted.

One can deduce from the figure that an increase in electric vehicles is accompanied by a decrease in the voltage across the nodes, reflecting a voltage drop experienced by the cables due to increased consumption. In contrast, an increase in PV systems leads to a higher voltage level, exceeding 1 p.u. It should be noted that this phenomenon is limited by the fact that the BESS is designed for SC and therefore prevents this effect. It is important to note that for the chosen network, the voltage is still within limits, despite the 7.4 kW charging rate. However, this needs to be nuanced as the individual annual consumption is limited to 5000 kWh and the cable cross section of the network is 4×150 mm^2. Consequently, it indicates that an EV-rich scenario is likely to cause voltage issues, as demonstrated in [21]. Nevertheless, an assessment of this is not part of the intended scope of this study.

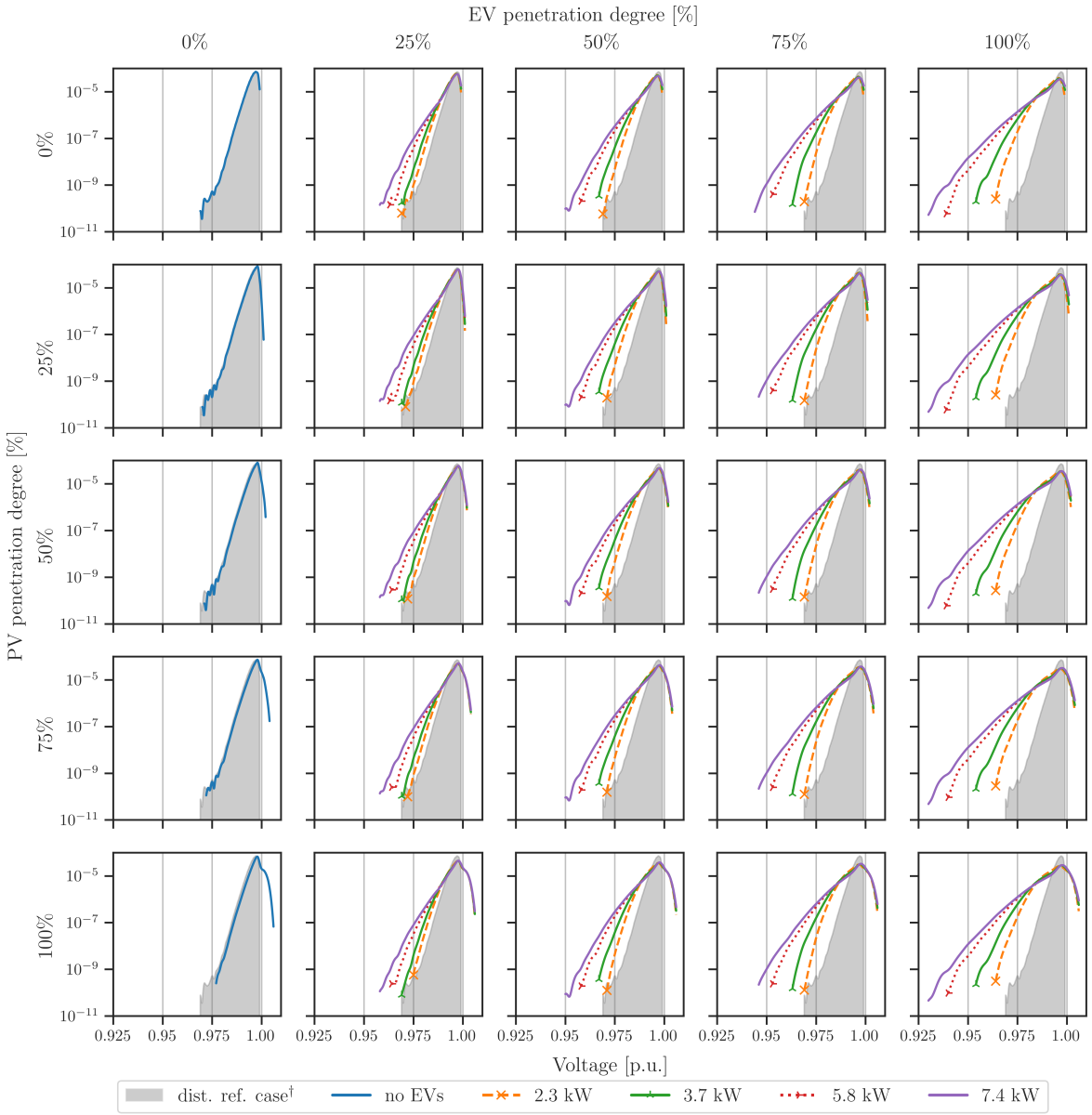

Figure 3. Gaussian distribution of the voltage profiles for different EV and PV levels at various charging rates; † the grey shaded zone denotes the 0% EV and 0% PV case.

4.2. Voltage Profiles — Partim DC

Given the fact that the MPPT is centralized in the LVDC backbone, distributed PV systems on the DC-branch will not operate on the same voltage (V_{pv}) operating point. Due to over- or undervoltage, the power operating point (P_{pv}) will be shifted away from the MPPT, leading to a lower production. As shown in Figure 4, this is especially noticeable for increasing cable lengths, where a power reduction of 5% is observed when having an overvoltage of 10%. However, due to the lower slope at the left side of the $P_{pv} = f(V_{pv})$ curve, the undervoltage has less impact on the production.

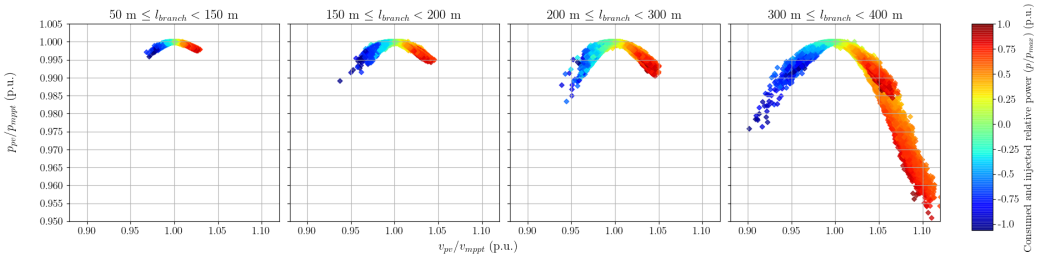

Figure 4. Voltage variation (V_{pv}) on the DC-branch and impact on the curtailed production (P_{pv}) as a function of the produced (positive) and consumed (negative) power.

4.3. Energy Losses

The bar charts in Figure 5 represent the different occurring losses in the two cases for the predefined scenarios. Results indicate that when having a combination of high EV and low PV penetration level, the benefits of an LVDC backbone decrease or even tend to be unfavourable. This becomes even more clear at higher charging rates (P_{ch}). As the PV systems cannot sufficiently cover the EV charging demand on the same DC-branch, power is taken from other DC-branches, the BESS or the AC grid, leading to an increase of conversion losses in the DC/AC and DC/DC converters of the DC-branch.

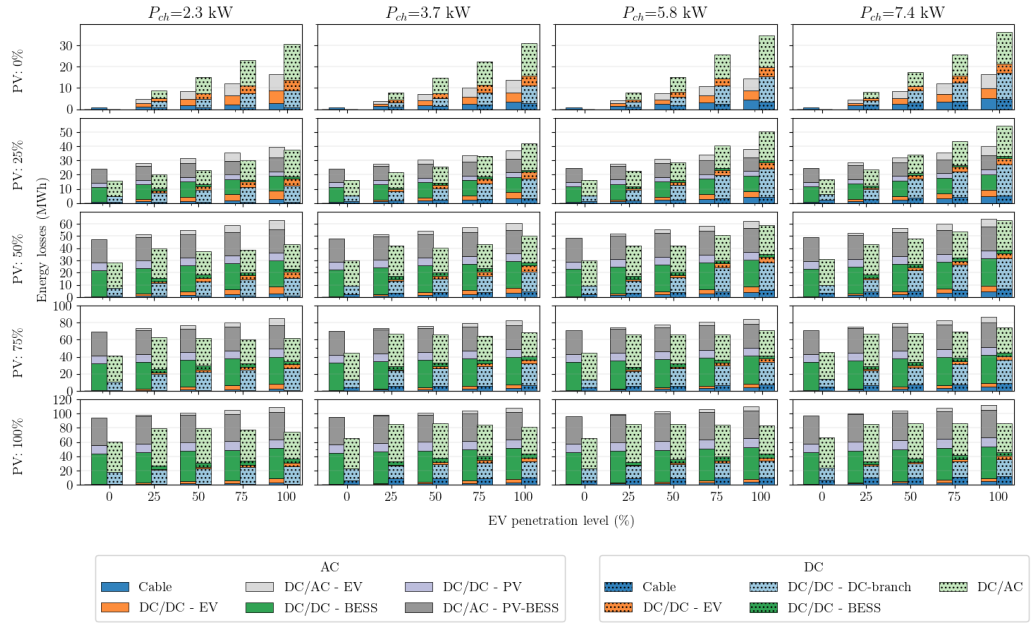

Figure 5. Conversion and cable losses for different EV charging powers and PV penetration levels for a conventional LVAC grid and the proposed LVDC backbone.

The higher the PV penetration level is, the smaller the increase rate of the losses for the LVDC backbone as a function of the EV penetration level will be. Although the conversion losses of the DC/DC at the DC-branch increase, the opposite trend is visible for the DC/AC conversion losses. This can be explained by the fact that a higher EV penetration level leads to a better SC and simultaneously an increasing energy exchange between the several DC-branches and the BESS.

This consequently means that as the losses for the AC case still increase, the benefit of an LVDC backbone increases in EV and PV rich scenarios. Figure 6 represents the relative energy loss difference ($RELD$) given in Equation (11) and clearly exhibits this behaviour.

$$RELD = \frac{E_{loss,dc} - E_{loss,ac}}{E_{loss,ac}} \tag{11}$$

with $E_{loss,dc}$ and $E_{loss,ac}$ as the accumulated losses occurring in the AC and DC cases. Similar behaviour can be observed at PV penetration levels 50% and 75%. However, the $RELD$ stagnates at those levels, before it decreases again. A further increase of the EV penetration leads in this situation to an increase in the power extracted from the grid. Finally, the threshold in EV penetration level where the DC approach becomes unfavourable decreases as a function of the increasing charging power.

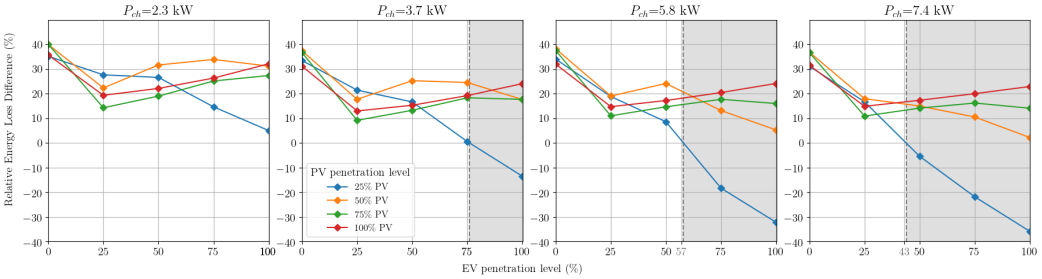

Figure 6. Comparison of the losses between the conventional approach and the proposed LVDC backbone for different charging rates, EV and PV penetration levels.

In Table 4, the feed-out energy from the grid is given for different charging powers for the case with 100% penetration of EV and PV. The relative feed-out energy difference ($RFOED$) given in Equation (12) denotes the difference in self-sufficiency between the conventional AC system and the proposed LVDC backbone. This indicator is represented as a function of the feed-out energy from the AC ($E_{FOE,dc}$) and DC ($E_{FOE,ac}$) case:

$$RFOED = \frac{E_{FOE,ac} - E_{FOE,dc}}{E_{loss,ac}} \tag{12}$$

A substantial decrease of the $RFOED$ is observed with higher charging powers caused by the reduced SC on the LVDC backbone. This is mainly the consequence of the increased cable losses.

Table 4. Feed-out energy from the grid for the 100% EV and 100% PV case.

$\mathbf{P_{ch}}$ **[kW]**	**2.3**	**3.7**	**5.8**	**7.4**
AC [MWh]	374.448	374.184	376.151	377.885
DC [MWh]	329.347	331.617	335.574	338.808
***RFOED* [%]**	12.04	11.38	10.79	10.34

4.4. Voltage Unbalance

A key indicator of the power quality within a DN, is given by the voltage unbalance factor (VUF) [41]. This measure is determined by symmetrical components as presented in Equations (13) and (14), where V_p and V_n represent the positive and negative sequences of the voltage phasors, respectively, while operator a represents a phase shift of 120 degrees (i.e., $1\angle 120°$):

$$V_p = \frac{V_a + a \cdot V_b + a^2 \cdot V_c}{3} \tag{13}$$

$$V_n = \frac{V_a + a^2 \cdot V_b + a \cdot V_c}{3} \tag{14}$$

If $|V_n|$ denotes the magnitudes of the negative sequence voltage and $|V_p|$ the positive sequence voltage, one describes the voltage unbalance factor as the ratio between them. In

accordance with the IEC EN 50160 standard [17], voltage unbalance may not exceed the limit of 2%:

$$VUF = \frac{|V_n|}{|V_p|} \cdot 100, \qquad \textbf{where } VUF \leq 2\% \tag{15}$$

Results of the VUF are shown in Figure 7, where the voltage unbalance of all the nodes is represented in relation to the losses each node experiences. Here, the figure is valid for the implementation of EVs (charged at 7.4 kW) into the grid without PV systems connected. Figure 7a represents the reference case without EVs, Figure 7b the 50% EV penetration scenario and Figure 7c a 100% case. A remarkable aspect in the figure is the correlation between the degree of voltage unbalance and the proportion of energy losses occurring on the DN. The same phenomenon is noticeable with lower EV penetration degrees, although the amplitude of VUF and node losses is more limited. Similarly, in case of even higher EV penetration, the limit will be reached more quickly.

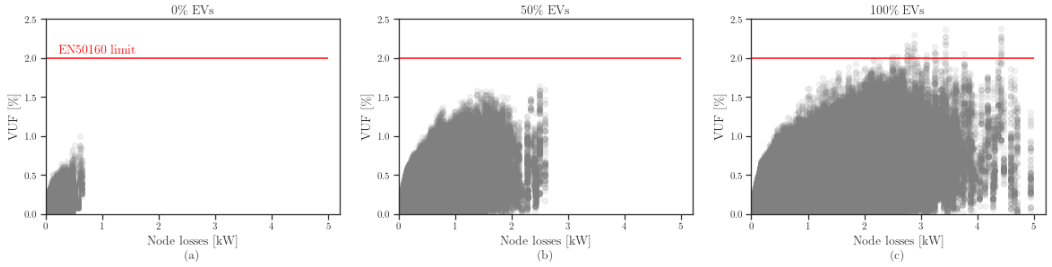

Figure 7. Voltage unbalance as a function of the node losses for various EV penetrations without PV systems, with: (**a**) 0% EV penetration; (**b**) 50% EV penetration; (**c**) 100% EV penetration.

Regarding the proposed LVDC backbone, it can be deduced from Figure 7 that the reference case applies. Thus, introducing an LVDC backbone involves as the main advantage that the DN will not be affected by voltage unbalances for penetration reaching up to 100%.

4.5. Results Discussion

As a result of the conducted analyses, several key observations were identified:

- No violation of the voltage limit was observed in the AC part. This was highly expected for the case with PV systems since the coupled BESS ensures that the injection is limited. However, when exclusively EVs are connected, the occurring voltage drop strongly depends on the load capacity on the one hand and on the presence or absence of a PV system on the other hand. In the case of 100% penetration of EVs with a 7.4 kW charging rate, the minimum voltage level observed is 0.92 p.u., corresponding to 211 V.
- The directly connected PV systems on the DC-branches increase the SC by the locally distributed EV chargers. However, a drawback of this architecture is that a voltage drop or rise leads to a reduction in power, going up to 5% for longer cable lengths. Nevertheless, an undervoltage caused by a high simultaneity of EV charging leads to a limited power reduction of 2.5%. This can be explained by the fact that during undervoltage, the PV systems operate on the left side of the maximum power which has a lower slope than on the right side.
- Comparing the absence of electric vehicles with the systematic introduction of EVs (i.e., in steps of 25%), one notices that the energy losses associated with charging not only cause higher losses but reveal a linear relationship with the voltage imbalance within the DN. Furthermore, the study demonstrates that from integration levels of 75% and onwards, voltage unbalance violations of the EN 50160 standard are recorded. Consequently, a considerable advantage of unipolar LVDC backbones manifests itself in the absence of voltage unbalance. Therefore, higher levels of EVs can be connected to the DN without causing predominant losses.
- The benefit of an LVDC backbone compared to a conventional AC system is especially observed when the stored BESS and PV energy can be consumed within the DC

system. Hence, it is important that a high EV penetration is accompanied with a certain penetration level of PV systems and BESS. Results also demonstrated that the charging power is an important parameter, whereas the higher the charging power, the lower the EV penetration level threshold for which the LVDC backbone becomes unfavourable. The amount of energy withdrawn from the grid reduces by almost 12% when the proposed LVDC backbone is applied.

5. Conclusions

In this paper, we presented a framework for charging electric vehicles on a hybrid AC/DC microgrid, i.e., LVDC backbone. Using the proposed backbone, we demonstrated that voltage profiles were maintained within the limits while experiencing less variations. Based on the results, we conclude that implementing an LVDC backbone reduces the voltage unbalance and voltage magnitude fluctuations across the low-voltage distribution network, thus helping mitigate the power quality disturbances on the AC-side of the hybrid microgrid. Nonetheless, the power flows are more volatile as the PV systems are directly connected on the DC-branches. Hereby, an extensive assessment of the converter and cable losses was performed, revealing that the present work reduces the amount of converter stages in the microgrid and improves the converter efficiencies. The results of the case study on a residential low-voltage radial distribution grid with different levels of electric vehicles and photovoltaic systems penetration confirmed the effectiveness of the proposed framework. Implications of these scenarios are significant for studies of hybrid microgrids: the degree of electric vehicle and photovoltaic system integration have a significant impact on whether the network's losses are compensated or increasing combined with the used charging rate. However, it is important to note that the simulations do not incorporate harmonic distortion, which qualifies as an interesting subject matter for future studies. Incorporating these harmonics (i.e., switching frequency harmonics) could influence the obtained results in terms of both the voltage stability and the loss terms, which would return more realistic results. Another interesting direction for further research is to incorporate a coordinated charging or vehicle-to-grid algorithm into the model. This could further evaluate the benefits of an LVDC backbone in terms of voltage stability, increased efficiency and cost savings.

6. Future Research and Discussions

The authors plan to perform further investigations on the impact of EVs, PV systems and BESS on the distribution grid. DC voltage levels and dynamic voltage control are also the subject of further optimisation. An article was submitted investigating the benefits of applying a dynamic voltage on an LVDC backbone with converterless PV and BESS [42]. Results were promising, exhibiting huge potential for the reduction of energy losses. This analysis will be extended by including distributed EV chargers, thereby attaining an efficient energy system with simpler PV integration and increased hosting capacity. Moreover, an economic and environmental analysis will be conducted to provide insights into the viability of LVDC for grid planners and operators, aimed at bridging the gap between current DNs and future low-voltage DC microgrids. Finally, the influence of massive EV penetration on the zero sequence voltage unbalance will be assessed since current standards impose no limits. In addition, the impact of harmonic distortion on the obtained voltage magnitudes and the voltage stability will also be a subject of future research.

Author Contributions: Conceptualization, R.C. and H.A.; methodology, R.C. and H.A.; software, R.C. and H.A.; validation, R.C. and H.A.; formal analysis, R.C. and H.A.; data curation, R.C. and H.A.; writing—original draft preparation, R.C. and H.A.; writing—review and editing, M.V., T.C. and J.D.; visualization, R.C. and H.A.; supervision, J.D.; project administration, J.D.; funding acquisition, J.D. All authors have read and agreed to the published version of the manuscript.

Funding: This research received no external funding.

Data Availability Statement: The used consumption profiles and grid data were obtained through a non-disclosure agreement, and therefore can not be shared.

Acknowledgments: We thank Fluvius cvba. for providing the dataset of consumption profiles and the grid data. Secondly, the authors would equally like to thank the (Belgian) Royal Meteorological Institute for providing the meteorological data, used for the calculation of PV system model.

Conflicts of Interest: The authors declare no conflict of interest.

Abbreviations

The following abbreviations are used in this manuscript:

BESS	Battery Energy Storage System
CC	Constant current
CV	Constant voltage
DN	Distribution Networks
EV	Electric Vehicle
LVDC	Low-voltage Direct Current
MPP	Maximum Power Point
MPPT	Maximum Power Point Tracking
PCC	Point of Common Coupling
PV	Photovoltaic
RELD	Relative Energy Loss Difference
RES	Renewable Energy Sources
RFOED	Relative Feed-out Energy Difference
SC	Self-consumption
SDGE	Stochastic Distribution Grid Exchangers
SoC	State of Charge
SPoC	Single Point of Connection
VUF	Voltage Unbalance Factor

References

1. Monteiro, V.; Gonçalves, H.; Afonso, J.a.L. Impact of Electric Vehicles on power quality in a Smart Grid context. In Proceedings of the 11th International Conference on Electrical Power Quality and Utilisation, Lisbon, Portugal, 17–19 October 2011; pp. 1–6. [CrossRef]
2. Lopes, J.a.A.P.; Soares, F.J.; Almeida, P.M.R. Integration of Electric Vehicles in the Electric Power System. *Proc. IEEE* **2011**, *99*, 168–183. [CrossRef]
3. Apostolaki-Iosifidou, E.; Codani, P.; Kempton, W. Measurement of power loss during electric vehicle charging and discharging. *Energy* **2017**, *127*, 730–742. [CrossRef]
4. Rönnberg, S.; Bollen, M. Power quality issues in the electric power system of the future. *Electr. J.* **2016**, *29*, 49–61. [CrossRef]
5. Leemput, N.; Geth, F.; Van Roy, J.; Delnooz, A.; Büscher, J.; Driesen, J. Impact of Electric Vehicle On-Board Single-Phase Charging Strategies on a Flemish Residential Grid. *IEEE Trans. Smart Grid* **2014**, *5*, 1815–1822. [CrossRef]
6. Ploumpidou, E. Supporting the Transition to DC Micro Grids in the Built Environment. Ph.D. Thesis, Technische Universiteit Eindhoven, Eindhoven, The Netherlands, 2017.
7. Yang, S.; Bryant, A.; Mawby, P.; Xiang, D.; Ran, L.; Tavner, P. An industry-based survey of reliability in power electronic converters. *IEEE Trans. Ind. Appl.* **2011**, *47*, 1441–1451. [CrossRef]
8. Rekola, J. Factors Affecting Efficiency of LVDC Distribution Network–Power Electronics Perspective. Ph.D. Thesis, Tampere University of Technology, Tampere, Finland, 2015.
9. Azaioud, H.; Claeys, R.; Knockaert, J.; Vandevelde, L.; Desmet, J. A Low-Voltage DC Backbone with Aggregated RES and BESS: Benefits Compared to a Traditional Low-Voltage AC System. *Energies* **2021**, *14*, 1420. [CrossRef]
10. Kabus, M.; Nolting, L.; Mortimer, B.J.; Koj, J.C.; Kuckshinrichs, W.; De Doncker, R.W.; Praktiknjo, A. Environmental impacts of charging concepts for battery electric vehicles: A comparison of on-board and off-board charging systems based on a life cycle assessment. *Energies* **2020**, *13*, 6508. [CrossRef]
11. Huynh, W.; Hoang, T.; Abhisek, U.; Nirmal-Kumar C.N. Comparison of Low-Voltage AC and DC Distribution Networks for EV Charging. In Proceedings of the 2022 7th IEEE Workshop on the Electronic Grid (eGRID), Auckland, New Zealand, 29 November–2 December 2022; pp. 1–5. [CrossRef]
12. Konstantinos, S.; Gonçalves, J.E.; Saelens, D.; Baert, K.; Driesen, J. Electrical system architectures for building-integrated photovoltaics: A comparative analysis using a modelling framework in Modelica. *Appl. Energy* **2020**, *261*, 114247. [CrossRef]

13. Gerber, D.L.; Vossos, V.; Feng, W.; Marnay, C.; Nordman, B.; Brown, R. A simulation-based efficiency comparison of AC and DC power distribution networks in commercial buildings. *Appl. Energy* **2018**, *210*, 1167–1187. [CrossRef]
14. Hernández, J.C. and Ruiz-Rodriguez, F.J. and Jurado, F. Modelling and assessment of the combined technical impact of electric vehicles and photovoltaic generation in radial distribution systems. *Energy* **2017**, *141*, 316–332. [CrossRef]
15. Brinkel, N.; Gerritsma, M.; AlSkaif, T.; Lampropoulos, I.; van Voorden, A.; Fidder, H.; van Sark, W. Impact of rapid PV fluctuations on power quality in the low-voltage grid and mitigation strategies using electric vehicles. *Int. J. Electr. Power Energy Syst.* **2020**, *118*, 105741. [CrossRef]
16. Fachrizal, R.; Ramadhani, H.; Munkhammar, J.; Widén, J. Combined PV–EV hosting capacity assessment for a residential LV distribution grid with smart EV charging and PV curtailment. *Sustain. Energy Grids Netw.* **2021**, *26*, 100445. [CrossRef]
17. *EN 50160:2011*; Voltage Characteristics of Electricity Supplied by Public Distribution Networks. IEC: Geneva, Switzerland, 2011.
18. Masoum, M.A.; Moses, P.S.; Hajforoosh, S. Distribution transformer stress in smart grid with coordinated charging of Plug-In Electric Vehicles. In Proceedings of the 2012 IEEE PES Innovative Smart Grid Technologies (ISGT), Washington, DC, USA, 16–22 January 2012; pp. 1–8. [CrossRef]
19. De Hoog, J.; Alpcan, T.; Brazil, M.; Thomas, D.A.; Mareels, I. Optimal Charging of Electric Vehicles Taking Distribution Network Constraints Into Account. *IEEE Trans. Power Syst.* **2015**, *30*, 365–375. [CrossRef]
20. Gemassmer, J.; Daam, C.; Reibsch, R. Challenges in Grid Integration of Electric Vehicles in Urban and Rural Areas. *World Electr. Veh. J.* **2021**, *12*, 206. [CrossRef]
21. Held, L.; Märtz, A.; Krohn, D.; Wirth, J.; Zimmerlin, M.; Suriyah, M.R.; Leibfried, T.; Jochem, P.; Fichtner, W. The Influence of Electric Vehicle Charging on Low Voltage Grids with Characteristics Typical for Germany. *World Electr. Veh. J.* **2019**, *10*, 88. [CrossRef]
22. Bhattacharyya, S.; Wijnand, M.; Slangen, T. Estimating the future impact of residential EV loads on low voltage distribution networks. In Proceedings of the CIRED Porto Workshop 2022: E-mobility and power distribution systems, Porto, Portugal, 2–3 June 2022; pp. 128–132. [CrossRef]
23. Marah, B.; Bhavanam, Y.; Taylor, G.; Ekwue, A. Impact of electric vehicle charging systems on low voltage distribution networks. In Proceedings of the 2016 51st International Universities Power Engineering Conference (UPEC), Coimbra, Portugal, 6–9 September 2016; pp. 1–6. [CrossRef]
24. Alame, D.; Azzouz, M.; Kar, N. Assessing and mitigating impacts of electric vehicle harmonic currents on distribution systems. *Energies* **2020**, *13*, 3257. [CrossRef]
25. Khaligh, A.; D'Antonio, M. Global Trends in High-Power On-Board Chargers for Electric Vehicles. *IEEE Trans. Veh. Technol.* **2019**, *68*, 3306–3324. [CrossRef]
26. Synergrid. *Technical Prescription C10/11—Specific Technical Prescriptions Regarding Power-Generating Plants Operating in Parallel to the Distribution Network*; Synergrid: Brussels, Belgium, 2019.
27. Claeys, R.; Azaioud, H.; Cleenwerck, R.; Knockaert, J.; Desmet, J. A Novel Feature Set for Low-Voltage Consumers, Based on the Temporal Dependence of Consumption and Peak Demands. *Energies* **2021**, *14*, 139. [CrossRef]
28. Claeys, R.; Delerue, T.; Desmet, J. Assessing the influence of the aggregation level of residential consumers through load duration curves. In Proceedings of the 2019 IEEE PES Innovative Smart Grid Technologies Europe (ISGT-Europe), Bucharest, Romania, 29 September–2 October 2019; pp. 1–5. [CrossRef]
29. Elaad N.L. Data Analytics. Available online: www.elaad.nl/research/data-analytics/ (accessed on 24 February 2022).
30. Pelletier, S.; Jabali, O.; Laporte, G.; Veneroni, M. Battery degradation and behaviour for electric vehicles: Review and numerical analyses of several models. *Transp. Res. B: Methodol.* **2017**, *103*, 158–187. [CrossRef]
31. Tremblay, O.; Louis-A., D.; Dekkiche, A.I. A Generic Battery Model for the Dynamic Simulation of Hybrid Electric Vehicles. In Proceedings of the 2007 IEEE Vehicle Power and Propulsion Conference, Arlington, TX, USA, 9–12 September 2007; pp. 284–289. [CrossRef]
32. Villalva, M.G.; Gazoli, J.R.; Filho, E.R. Comprehensive Approach to Modeling and Simulation of Photovoltaic Arrays. *IEEE Trans. Power Electron.* **2009**, *24*, 1198–1208. [CrossRef]
33. King, D.; Boyson, W.; Kratochvill, J. *Photovoltaic Array Performance Model*; Technical Report; Sandia National Lab: Albuquerque, NM, USA, 2004.
34. Azaioud, H.; Desmet, J.; Vandevelde, L. Benefit Evaluation of PV Orientation for Individual Residential Consumers. *Energies* **2020**, *13*, 5122. [CrossRef]
35. Li, K.; Tseng, K.J. Energy efficiency of lithium-ion battery used as energy storage devices in micro-grid. In Proceedings of the IECON 2015—41st Annual Conference of the IEEE Industrial Electronics Society, Yokohama, Japan, 9–12 November 2015; pp. 005235–005240. [CrossRef]
36. Trichakis, P.; Taylor, P.; Cipcigan, L.; Lyons, P.; Hair, R.; Ma, T. An Investigation of Voltage Unbalance in Low Voltage Distribution Networks with High Levels of SSEG. In Proceedings of the 41st International Universities Power Engineering Conference, Newcastle Upon Tyne, UK, 6–8 September 2006; pp. 182–186. [CrossRef]
37. Dugan, R.C.; McDermott, T.E. An open source platform for collaborating on smart grid research. In Proceedings of the 2011 IEEE Power and Energy Society General Meeting, Detroit, Michigan, USA, 24–29 July 2011; pp. 1–7. [CrossRef]
38. Hariri, A.; Newaz, A.; Faruque, O. Open-source python-OpenDSS interface for hybrid simulation of PV impact studies. *IET Gener. Trans. Distrib.* **2017**, *11*, 3125–3133. [CrossRef]

39. Cleenwerck, R.; Azaioud, H.; Claeys, R.; Coosemans, T.; Knockaert, J.; Desmet, J. An approach to the impedance modelling of low-voltage cables in digital twins. *Electr. Power Syst. Res.* **2022**, *210*, 108075. [CrossRef]
40. Fluvius. Heb Je Nood Aan 400V Om Je Elektrische Auto Op Te Laden? Available online: www.fluvius.be/sites/fluvius/files/2020-10/brochure-heb-je-nood-aan-400v-om-je-elektrischeauto-op-te-laden.pdf (accessed on 16 February 2022).
41. Girigoudar, K.; A. Roald, L. On the impact of different voltage unbalance metrics in distribution system optimization. *Electr. Power Syst. Res.* **2020**, *189*, 106656. [CrossRef]
42. Azaioud, H.; Farnam, A.; Knockaert, J.; Vandevelde, L.; Desmet, J. Efficiency optimisation and converterless PV integration by applying a dynamic voltage on an LVDC backbone. 2023; *submitted*.